Entropy of seismic electric signals: Analysis in natural time under time reversal

P. A. Varotsos,[1,2,*] N. V. Sarlis,[1] E. S. Skordas,[1,2] H. K. Tanaka,[3] and M. S. Lazaridou[1]
[1]*Solid State Section, Physics Department, University of Athens, Panepistimiopolis, Zografos 157 84, Athens, Greece*
[2]*Solid Earth Physics Institute, Physics Department, University of Athens, Panepistimiopolis, Zografos 157 84, Athens, Greece*
[3]*Earthquake Prediction Research Center, Tokai University 3-20-1, Shimizu-Orido, Shizuoka 424-8610, Japan*
(Received 16 April 2005; revised manuscript received 15 December 2005; published 27 March 2006)

Electric signals have been recently recorded at the Earth's surface with amplitudes appreciably larger than those hitherto reported. Their entropy in natural time is smaller than that of a "uniform" distribution. The same holds for their entropy upon time reversal. Such a behavior, which is also found by numerical simulations in fractional Brownian motion time series and in an on-off intermittency model, stems from infinitely ranged long range temporal correlations and hence these signals are probably seismic electric signal activities (critical dynamics). This classification is strikingly confirmed since three strong nearby earthquakes occurred (which is an extremely unusual fact) after the original submission of the present paper. The entropy fluctuations are found to increase upon approaching bursting, which is reminiscent of the behavior identifying sudden cardiac death individuals when analyzing their electrocardiograms.

DOI: 10.1103/PhysRevE.73.031114 PACS number(s): 91.30.Dk, 05.40.−a, 05.45.Tp, 87.19.Nn

I. INTRODUCTION

The time series analysis of various phenomena in complex systems (and especially those associated with impending catastrophic events, e.g., [1,2]) in the framework of the newly defined time domain [3,4], termed natural time, reveals interesting features. Examples are electrocardiograms [5,6], seismicity [3,7] and seismic electric signal (SES) activities [3,4,8–11]. This new time domain is optimal for enhancing the signals in time-frequency space when employing the Wigner function and measuring its localization property [12]; in other words natural time analysis conforms to the desire to reduce uncertainty and extract signal information as much as possible [12].

In a time series comprising N events, the natural time $\chi_k=k/N$ serves as an index [3,4] for the occurrence of the kth event. It is, therefore, smaller than, or equal to, unity. In natural time analysis, the time evolution of the pair of the two quantities (χ_k, Q_k) is considered, where Q_k denotes in general a quantity proportional to the energy released during the kth event. For example, in the case of dichotomous electric signals [3,4,8,9] Q_k stands for the duration of the kth pulse. As a second example we refer to the analysis of seismicity [3,7], where Q_k is proportional to the seismic energy released during the kth earthquake (which is proportional to the seismic moment M_0 that is directly related to the earthquake magnitude). The entropy S in the natural time domain is defined [9] as the derivative of the function $\langle\chi^q\rangle-\langle\chi\rangle^q$ with respect to q, for $q=1$, which gives [3,9]

$$S \equiv \langle \chi \ln \chi \rangle - \langle \chi \rangle \ln \langle \chi \rangle, \tag{1}$$

where $\langle f(\chi)\rangle=\Sigma_{k=1}^{N} p_k f(\chi_k)$ and $p_k=Q_k/\Sigma_{n=1}^{N} Q_n$. It is a dynamic entropy depending on the sequential order of events [5,6] and exhibits [10] concavity, positivity, and Lesche [13,14] stability. When the system enters the critical stage (infinitely ranged long range temporal correlations [3,4]), the S value is smaller [9,11] than the value $S_u(=1/2\ln 2-1/4 \approx 0.0966)$ of a "uniform" distribution (defined in Refs. [3,5,6,9], e.g., when all p_k are equal), i.e.,

$$S < S_u. \tag{2}$$

The value of the entropy obtained upon considering the time reversal $\mathcal{T}$, i.e., $\mathcal{T}p_k=p_{N-k+1}$, is labeled by S_-. An important point which emerged from the data analysis in Ref. [10] is the following: Although the study of the S values enables the distinction between SES activities and noises produced by nearby operating artificial (manmade) electromagnetic sources (AN), i.e., $S<S_u$ for the SES activities and $S \gtrapprox S_u$ for AN, this does not hold for the S_- values. This is so, because for the SES activities we found that the S_- values are smaller than (or equal to) S_u, while for AN the S_- values are either smaller or larger than S_u. (This happens *in addition to* the fact that for the SES activities [3,4] the variance $\kappa_1 \equiv \langle\chi^2\rangle - \langle\chi\rangle^2$ is $\kappa_1 \approx 0.070$, while for AN we have [3,8,9] $\kappa_1 \geqslant 1/12$.) Here, we provide more recent data on the SES activities, which strengthen the conclusion that both S and S_- are smaller than S_u. In other words, the following key point seems to hold: In signals that exhibit critical dynamics (e.g., SES activities) upon time reversal their entropy values (though *different* than those in forward time) still remain smaller than S_u. Why? The answer to this question is a challenge, because, if it is generally so, among similar looking signals we can distinguish (cf. by means of the quantities κ_1, S, S_-) those that exhibit critical dynamics. Since the latter signals are expected to exhibit infinitely ranged long range correlations, this might be the origin of the aforementioned behavior. To investigate this point, numerical simulations are presented here for both fractional Brownian motion (fBm) time series as well as for an on-off intermittency model. These two numerical models are studied here for the following reasons:

*Electronic address: pvaro@otenet.gr

The simple case of an fBm is selected in view of the following suggestion forwarded in Ref. [8] as far as the Hurst exponent H is concerned. If we assume that, in general, H is actually a measure of the intensity of long range dependence, we may understand why the SES activities, when analyzed in the natural time domain, lead to H values close to unity, while AN (where the long range correlations are weaker [8]) to markedly smaller H values, e.g., around 0.7 to 0.8. As for the seismicity, it has been recently suggested [15] that "the Californian earthquakes are long-range temporal correlated according to the persistence of a fractal Gaussian *intermittent noise* with $H \approx 1$ known as $1/f$ or pink noise." Note, however, that there is still an ongoing discussion (see also [16]) on which dynamic model is appropriate for earthquakes (EQs). For example, we refer to the following two points: First, as far as the question on whether EQs are phenomena that are consistent with the self-organized criticality (SOC) aspect [17,18], Yang *et al.* [19] recently argued that EQs are unlikely phenomena of SOC because the analysis of the Southern California Catalog shows that the first-return-time probability $P_M(T)$ for EQs with a magnitude equal to or larger than some prescribed threshold M, is changed after rearranging the time series. To the contrary, Woodard *et al.* [20] expressed the view that the results of Yang *et al.*, far from discarding SOC for modeling earthquake dynamics, provide further evidence in favor of such a description (however, Yang *et al.* [21] subsequently insisted on the correctness of their initial conclusion [19]). Second, instead of SOC, the *intermittent criticality* model has been proposed [22] as being more appropriate (see also Refs. [23,24]). In order to proceed to a distinction between these two competing models, it has been stated [25] that a more precise definition of the two paradigms is needed. Since, however, recent studies [26] suggest that the EQ data support the intermittent criticality aspect, we restrict ourselves here to the presentation of the results of a simple on-off intermittency model.

The present paper is organized as follows: In Sec. II we present the most recent experimental data on electric signals along with their analysis in natural time and examine whether their S and S_- values are smaller than S_u. The values of S and S_- resulting from numerical simulations in the two models studied, i.e., fBm time-series and an on-off intermittency model, are given in Secs. III and IV, respectively. A short discussion follows in Sec. V, while in Sec. VI we summarize our main conclusions.

II. RECENT ELECTRIC SIGNALS AND THEIR ENTROPY IN NATURAL TIME

Figure 1 depicts five electric signals, labeled M_1, M_2, M_3, M_4, and V_1, that were recorded on 21 March 2005, 23 March 2005 and 7 April 2005. Each comprises a number of pulses (see Table I), an example of which is shown, for the sake of the reader's convenience, in Fig. 1(d). Note that the first four signals (M_1 to M_4)—recorded at a station labeled MYT lying in the northeastern Aegean sea [16]—have amplitudes that not only are one order of magnitude larger than the fifth one [V_1, see Fig. 1(c), recorded at a different station labeled VOL with a sampling frequency $f_{\text{exp}}=1$ Hz, see [16]], but also significantly exceed those hitherto reported [27]. Hence, from thereon we solely focus on the study of these four signals M_1, M_2, M_3, and M_4. The way they are read in natural time can be seen in Fig. 2. Their analysis leads to the S and S_- values given in Table I, an inspection of which reveals that they are actually smaller than S_u. Hence, on the basis of the aforementioned criterion, these signals (cf. for which it was *also* checked that their κ_1-values are close to $\kappa_1 = 0.070$) *cannot* be classified as AN, but they are likely to be SES activities. Note that, although in general S is different than S_-, no definite conclusion can be drawn on the sign of $S - S_-$ (see also Table I of Ref. [10]).

Beyond the aforementioned results of time series analysis, we now provide additional experimental evidence which supports the view that the signals M_1, M_2, M_3, and M_4 are (true) SES. The electric signals are *always* monitored by measuring the variations ΔV of the potential difference between (pairs of) electrodes—measuring dipoles—grounded at depths of ≈ 2 m. For the sake of noise discrimination, a multitude of dipoles is used as follows (e.g., [27,28]; for a review see Ref. [11]): Several dipoles are deployed usually along two directions (e.g., EW and NS) with lengths (L) between 50 and 300 m (*short* dipoles). In addition, longer dipoles, i.e., with L of the order of km, are simultaneously operating (*long* dipoles). In each of the Figs. 1(a) and 1(b) we show the recordings of two (out of eight) operating dipoles; one long dipole ($L \approx 1$ km), which is the upper channel in Figs. 1(a) and 1(b), and one short ($L \approx 300$ m, the lower channel) along the NS direction. The criteria to distinguish (true) SES from AN are the following (see Appendix 2 of Ref. [28]): The signals should appear at *both* the short dipoles and the long ones, which is actually observed in Figs. 1(a) and 1(b). Furthermore, for two *parallel* dipoles (of unequal length) their $\Delta V/L$ values should be the same. This can be clearly seen in Fig. 3, in which we show, as an example the $\Delta V/L$ values of two short dipoles directed along NS, the lower channel corresponds to $L \approx 300$ m [i.e., this is the *same* dipole with the lower one depicted in Figs. 1(a) and 1(b)] and the upper channel to $L \approx 150$ m. Note that, in contrast to Figs. 1(a) and 1(b) (each one of which depicts recordings with a total duration of the order of a few hours), Fig. 3 intentionally presents the recordings with a total duration of one week in order to show that the signals M_1, M_2, M_3, and M_4 are well above the (background) noise level cf. The electrodes of the two dipoles depicted in Fig. 3 are located at different sites, and hence the electrochemical influences—in the contacts between each electrode and the ground—are also different. This may explain the opposite trend of the two recordings seen in Fig. 3, which however, is disregarded since it does not obey the criterion $\Delta V/L \approx$ constant and moreover is excluded from our analysis, since only the duration of the pulses is involved, Fig. 1(d), see also p. 177 of Ref. [11], thus not affecting our results).

We now further comment on the extent of the objectivity of the (natural) time series analysis mentioned in the first paragraph of this section, which revealed that the signals M_1, M_2, M_3, and M_4 obey the S and S_- criterion. An SES activity has been defined [28] when *many* SESs (cf. each transient pulse is a single SES) of the *same* polarity are recorded

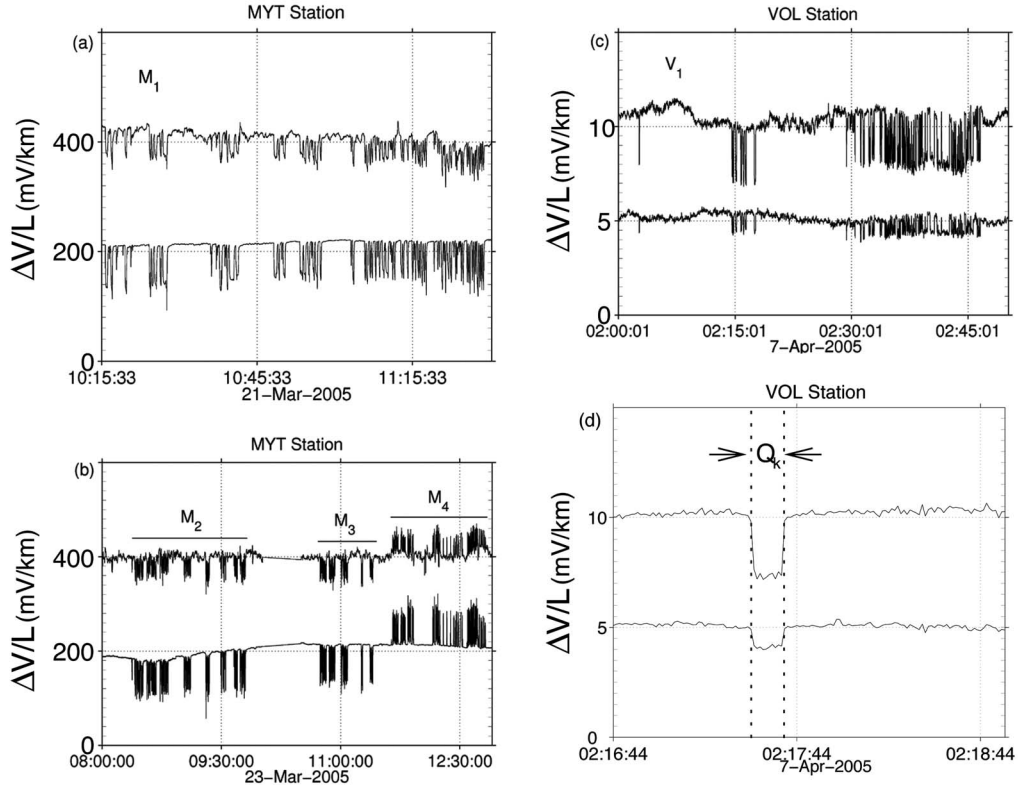

FIG. 1. Electric signals recorded on March 21, 2005 (a), March 23, 2005 (b), and April 7, 2005 (c). The signals in (a) and (c) are labeled hereafter M_1 and V_1, respectively, while that in (b) consists of the three signals activities labeled M_2, M_3, and M_4. The universal time is marked on the horizontal axis. Additional details for the two dipoles—records of which are shown here—as well as for the sites of the measuring stations are provided in Ref. [16]. All recordings for the sake of clarity are displaced vertically by constant factors. (d) is an excerpt of (c), showing—in an expanded time scale—an example of a pulse, i.e., the kth ($k=12$) pulse of V_1, and its duration Q_k (cf. the thick broken lines indicate the initiation and the cessation of the pulse).

within a relatively short time, i.e., with a total duration of the order of a few hours or so. Following this definition, a few pulses of opposite polarity that can be seen just before M_1 in Fig. 3 are discarded for further analysis since they do not constitute an SES activity. Furthermore, among the four signals M_1, M_2, M_3, and M_4 marked in Figs. 1(a) and 1(b), only two, i.e., M_1 and M_4, can be undoubtedly separated from the others (since M_1 was recorded on March 21 while the other three on March 23; further M_4 cannot be mixed with M_2, M_3 in view of their *opposite* polarities). On the other hand, as far as the signals M_2 and M_3 are concerned, an ambiguity emerges, because in principle they may belong to the same SES activity or may constitute separate SES activities. In view of these facts, the following steps were consecutively applied to our analysis in the natural time domain. We first analyzed M_1 and found that it obeys the criterion, i.e., S and S_- smaller than S_u. We then proceeded to the analysis of M_4 and found again that this criterion is fulfilled (recall that, the variance κ_1 was also calculated and, for each of these signals M_1 and M_4, resulted in a value close to 0.070). Finally, as a third step, we focused on the remaining recordings of March 23 (comprising M_2 and M_3). Considering the aforementioned ambiguity, we checked both possibilities that is (i) we analyzed M_2 and M_3 together and found that not only the criterion was violated but also the M_2+M_3 signal (altogether) behaved like a "uniform" distribution (cf. the corresponding κ_1 value was around $1/12$). (ii) On the other hand, if we analyze separately M_2 and M_3, they both obeyed the criterion (furthermore their κ_1 values resulted in values close to 0.070). The first possibility (if it were true) would reflect that the M_2+M_3 signal would be AN, which however, is in direct contrast to the additional experimental evidence mentioned in the previous paragraph, which revealed that all the signals M_1, M_2, M_3, and M_4 are (true) preseismic signals and not AN. Hence, we concluded that the second possibility is likely to be the true one.

TABLE I. The values of S and S_- together with the number of pulses N for the SES activities (the original time series have lengths between 2×10^3 and 10^4, compare Fig. 1 with $f_{\text{exp}}=1$ Hz) shown in Fig. 1. It has been also checked that in all these signals κ_1 is close to 0.070.

Signal	N	S	S_-
M_1	78±9	0.094±0.005	0.078±0.003
M_2	103±5	0.089±0.003	0.084±0.003
M_3	53±3	0.089±0.004	0.093±0.004
M_4	95±3	0.080±0.005	0.086±0.006
V_1	119±14	0.078±0.006	0.092±0.005

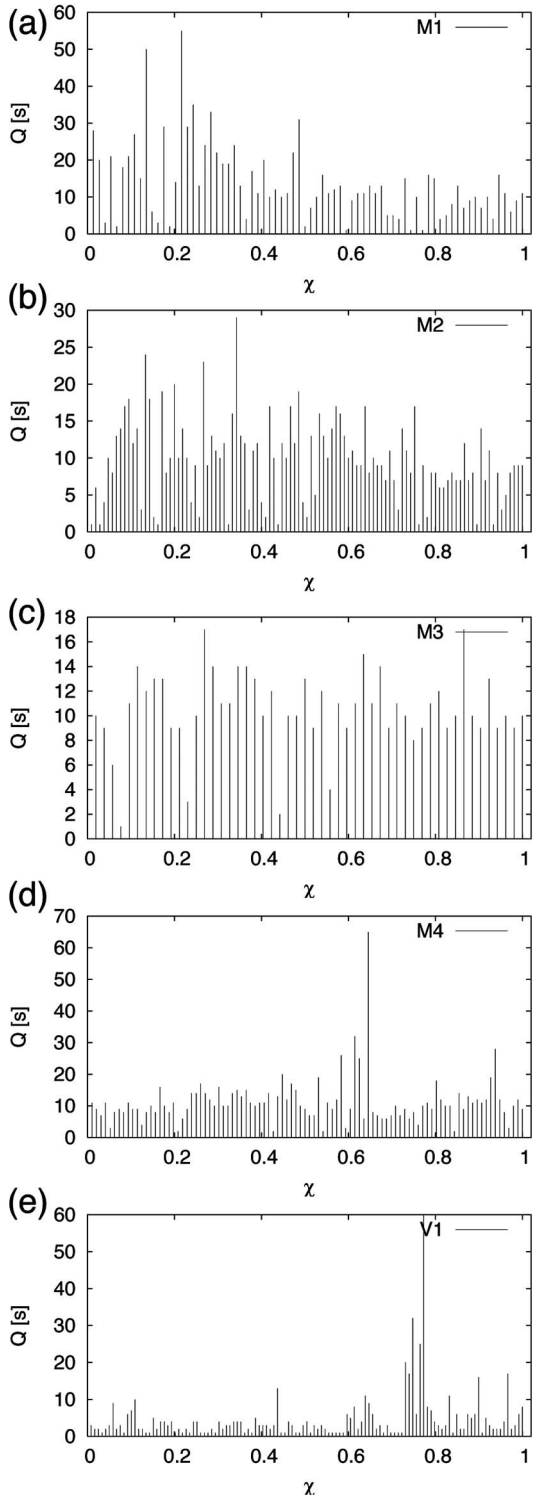

FIG. 2. How the signals depicted in Fig. 1 are read in natural time. (a), (b), (c), (d), and (e), correspond to the signals activities labeled M_1, M_2, M_3, M_4, and V_1, respectively.

III. FRACTIONAL BROWNIAN MOTION TIME SERIES: THE ENTROPY IN NATURAL TIME

We first clarify that Weron *et al.* [29] recently studied an algorithm distinguishing between the origins (i.e., the memory and the tails of the process) of the self-similarity of a given time series on the base of the computer test suggested in Ref. [30]. By applying it to the SES activities, they found the fBm as the appropriate type of modeling process. The fBm, which is H self-similar with stationary increments and it is [31] the only Gaussian process with such properties for $0<H<1$, can be simulated [32,33], (see also pp. 321–323 of Ref. [34]), by randomizing a construction due to Weierstrass, i.e., using the Weierstrass-Mandelbrot function [35]

$$w(t)=\sum_l c_l \frac{\sin(b^l t+d_l)}{b^{lH}}, \tag{3}$$

where $b>1$, c_l normally distributed with mean 0 and standard deviation 1, and d_l are uniformly distributed in the interval $[0,2\pi]$ (cf. when using the increments of Eq. (3) one can also produce fractional Gaussian noise of a given H).

By using Eq. (3), fBm for various values of H were produced, the one signed segments of which were analyzed in the natural time domain (an example is given in Ref. [16]). This means that if we denote by w_i, $i=0,1,2,\ldots N+1$, some $N+2$ consecutive fBm values obtained from Eq. (3) with $w_0 w_1<0$, $w_N w_{N+1}<0$ and all w_n, $n=1,2,\ldots N$ have the same sign—thus, constituting an one-signed segment—then the p_k, $k=1,2,\ldots N$ used in the calculation are given by p_k

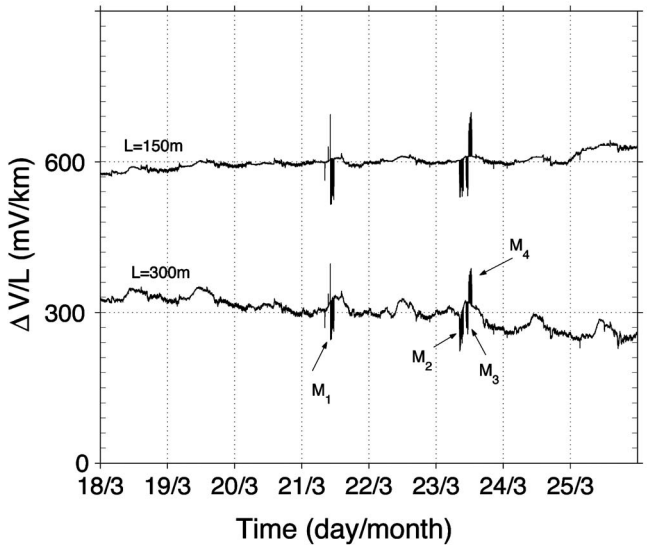

FIG. 3. The recordings of two parallel (short) dipoles (oriented along NS) operating at MYT for the period 18 March 2005 to 26 March 2005. These $\Delta V/L$ values plotted show that the electric signals M_1, M_2, M_3, and M_4 under discussion: (i) obey the criterion [28] $\Delta V/L \approx$ constant and (ii) are well above the background noise level. In order to better realize the latter, we intentionally depict here recordings that have a total duration of one week, while those in Figs. 1(a)–1(c) have an appreciably shorter total duration, i.e., a few hours each. The almost sinusoidal variations (with a period of almost 24 hours) of the background are mainly due to small variations of the magnetic field of the Earth (magnetotelluric variations), as verified by independent magnetic field measurements. Both recordings for the sake of clarity are displaced vertically by constant factors.

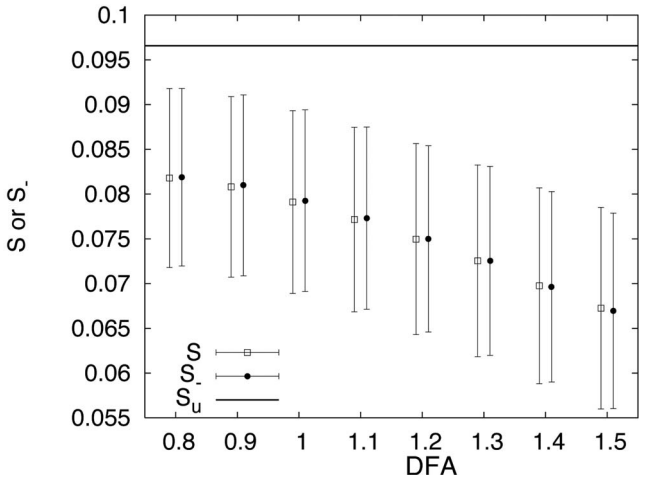

FIG. 4. Calculated values of S (squares) and S_- (circles) vs the DFA exponent α_{DFA}. The error bars indicate the region of one standard deviation ($\pm\sigma$). The horizontal line corresponds to S_u.

$=w_k/\Sigma_{n=1}^{N} w_n$ and correspond to the "durations" $Q_k=w_k$ mentioned in Sec. I. The Monte Carlo simulation results obtained for each one-signed segment include not only the values of the entropies S and S_-, but also the exponent α_{DFA} of the detrended fluctuation analysis (DFA) [36,37]. For segments of a small number of points N (cf. only segments with $N>40$ were considered), the values of α_{DFA} may vary significantly, but they scatter around that which is expected for a given value of H (see Fig. 11 of Ref. [8]); in this sense, the DFA exponent α_{DFA} is consistent with the H index used to generate fBm by means of Eq. (3). The method of DFA was preferred, because it is one of the few well defined and robust estimators of the scaling properties for such segments (e.g., [8], see also pp. 300–301 of Ref. [11]). The results are shown in Fig. 4, in which we plot the S and S_- values versus α_{DFA}. Since the analysis of the SES activities in natural time results in [8,9] DFA exponents α_{DFA} around unity, in Fig. 4 we are solely focused on the range $0.8<\alpha_{DFA}<1.2$. An inspection of this figure reveals the following three conclusions: First, despite the large standard deviation, we may say that both S and S_- are smaller than $S_u(\approx 0.0966)$ when $\alpha_{DFA}\approx 1$ (cf. interestingly, when plotting—instead of Fig. 4—the κ_1 value versus α_{DFA} we find that $\kappa_1\approx 0.070$ when $\alpha_{DFA}=1$). Second, S and S_- are more or less comparable. Third, comparing the computed S and S_- values (≈ 0.08 for $\alpha_{DFA}\approx 1$) with those resulting from the analysis of the SES activities (see Table I, see also Table I of Ref. [10]), we find a reasonable agreement. Note that these computations do *not* result in a definite sign for $S-S_-$ in a similar fashion with the experimental results.

IV. THE ENTROPY IN NATURAL TIME IN AN ON-OFF INTERMITTENCY MODEL

We clarify that on-off intermittency is a phase-space mechanism that allows dynamical systems to undergo bursting (bursting is a phenomenon in which episodes of high activity are alternated with periods of inactivity as in Fig. 2(e), which corresponds to the SES activity V_1). This mechanism is different from the well known Pomeau-Manneville scenario for the behavior of a system in the proximity of a saddle-node bifurcation [38]. Here, we use the simple model of the driven logistic map

$$X_{t+1}=A(Y_t)X_t(1-X_t), \tag{4}$$

where we assume that the quantity $A(Y_t)$ is *monotonic* function of Y_t and that $0\leqslant A\leqslant 4$ (cf. A is further specified below). The system has the invariant manifold $X=0$ and the level of its activity is measured by X_t [39]. In order to have the on-off mechanism in action, we make particular mention of the case of a noise-driven logistic map, with

$$A(Y_t)=A_0+\alpha Y_t, \tag{5}$$

where Y_t is δ-correlated noise which is uniformly distributed in the interval [0,1] and A_0 and α are parameters. In order to have $0\leqslant A\leqslant 4$, we assume [39] $A_0\geqslant 0$, $\alpha\geqslant 0$ and $A_0+\alpha\leqslant 4$. The relevant parameter plane for the noise-driven system of Eqs. (4) and (5) (as well as the parameter range for which the fixed point $X=0$ is stable) can be found in Fig. 1 of Ref. [39], while the description of the intermittent dynamics is given in Refs. [40–43]. Bursting is observed in the temporal evolution of X_t as the stability of the fixed point $X=0$ varies. Following Ref. [41], for $A_0=0$ there is a *critical* value $\alpha_c>1$, below which the system asymptotically tends to the fixed point $X=0$, without any sustained intermittent bursting. For this case, i.e., $A_0=0$, the value $\alpha_c=e\equiv 2.718\,28\ldots$ leads to on-off intermittency [39]. In the intermittent system under discussion, both the signal amplitude and the power spectrum resulted in [39] power-law distributions with low frequencies predominating in the power spectrum.

Several time-series have been produced for the above on-off intermittency model with the following procedure: The system was initiated at a time ($t_{in}=-200$) with a uniformly distributed value $X_{t_{in}}$ in the region [0,1], and then the mapping of Eqs. (4) and (5) was followed until N events will occur after $t=0$. The results for X_t, $t=1,2\ldots N$ were analyzed in natural time domain (i.e., $p_k=X_k/\Sigma_{t=1}^{N}X_t$, where X_k here corresponds to the "duration" Q_k mentioned in Sec. I) and the values of S and S_- have been determined. This was repeated 10^3 times for a given number, N, of events and the average values of S and S_- have been deduced. These values are plotted in Fig. 5(a) vs $(\alpha-e)N^{1/2}$. (The factor $N^{1/2}$ stems from finite size scaling effects, since for large values of N, e.g., $N>15\,000$, a scaling—reminiscent of a first order phase transition—was observed, details on which will be published elsewhere.) This figure reveals that as the *critical* value is approached from below, i.e., $\alpha\rightarrow e_-$, both S and S_- are smaller than S_u.

V. DISCUSSION

We start by giving a simple example, which may clarify the meaning of the entropy, the significance of whether it is smaller or larger than the one of a "uniform" distribution and finally how it is influenced by a time reversal. Let us study the influence of the effect of a linear trend. The influence of

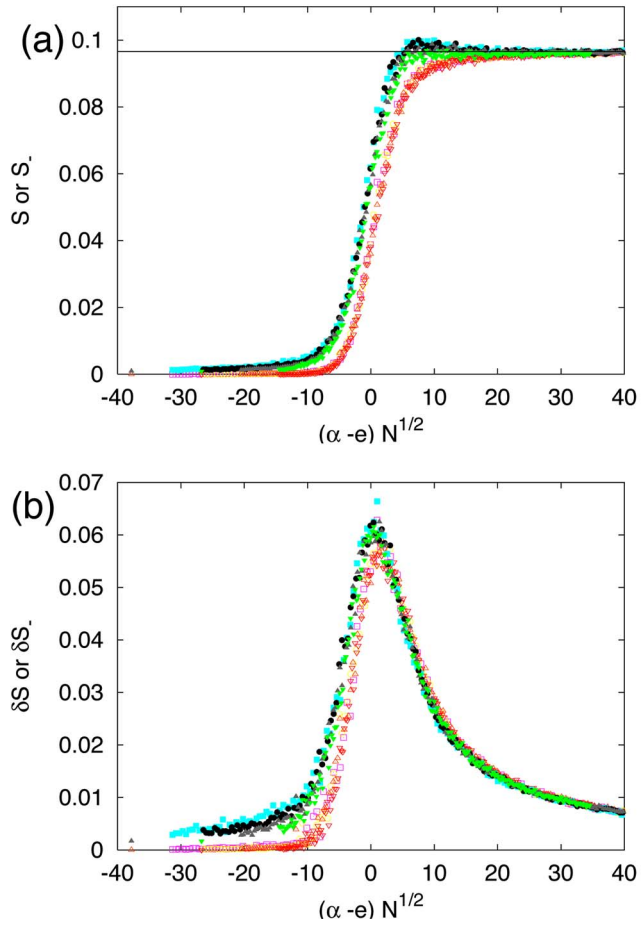

FIG. 5. (Color online) Calculated results for the on-off intermittency model discussed in the text. The average values of (a) S (closed symbols) and S_- (open symbols) and (b) the fluctuations δS and δS_- vs the finite size scaling variable $(\alpha-\alpha_c)N^{1/2}$. The quantity N stands for the number of the events considered in each sample time series; $N=70\,000$, 50 000, 30 000, and 15 000 correspond to squares, circles, triangles, and inverted triangles, respectively. The horizontal line in (a) corresponds to S_u.

a perturbative linear trend to the "uniform" distribution, $p(\chi)=1$, where $p(\chi)$ is a continuous probability density function (PDF) corresponding to the point probabilities p_k used so far, can be studied by means of the parametric family of PDFs: $p(\chi;\epsilon)=1+\epsilon(\chi-1/2)$ for *small* $\epsilon(<1)$. Such a family of PDFs shares the interesting property $\mathcal{T}p(\chi;\epsilon)=p(\chi;-\epsilon)$, i.e., the action of time reversal is obtained by simply changing the sign of ϵ. Moreover, the calculation of the entropy $S(\epsilon)\equiv S[p(\chi;\epsilon)]$, as well as that of the entropy under time reversal $S_-(\epsilon)\equiv S[\mathcal{T}p(\chi;\epsilon)]$, $S_-(\epsilon)=S(-\epsilon)$, can be done analytically, and the result yields

$$S(\epsilon)=-\frac{1}{4}+\frac{\epsilon}{72}-\left(\frac{1}{2}+\frac{\epsilon}{12}\right)\ln\left(\frac{1}{2}+\frac{\epsilon}{12}\right). \tag{6}$$

Figure 6 presents the values of S and S_- as a function of the linear trend parameter ϵ. We observe that they lie above and below S_u, respectively. In simple words, a (small) linearly increasing (decreasing) trend superimposed on a "uniform" distribution leads to an entropy S smaller (larger) than S_u, while S_- is larger (smaller) than S_u.

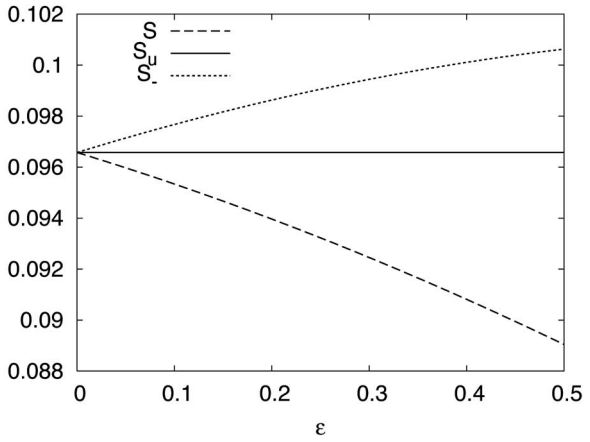

FIG. 6. The values of S (dashed) and S_- (dotted) as a function of the linear trend parameter ϵ. The solid line corresponds to S_u and is drawn for the sake of comparison.

We now turn to the computational results of Sec. III on a fBm time series, which showed that the DFA exponent $\alpha_{DFA}\approx 1$ corresponds to $S\approx S_-\approx 0.08$ and $\kappa_1\approx 0.070$. We first clarify that such a DFA exponent is consistent with the value $H\approx 1$ that resulted from the analysis of the SES activities in the natural time domain pointing at *critical* dynamics (infinitely long-ranged interactions) [8]. Further, we recall that the latter analysis of the SES activities also showed that their κ_1 values are [4] close to $\kappa_1\approx 0.070$ and their S values (as well as their S_- values) are on the average [8,10] around 0.08. In other words, the fBm computational results support the view that the values of H, κ_1, S, and S_- of SES activities stem from their infinitely ranged *temporal* correlations. This is also strengthened by the fact that, in the SES activities, upon *shuffling* the Q_k randomly (which destroys [5] the sequential order of the pulses and hence their time-correlations) the corresponding values change to $H\approx 0.5$, $\kappa_1\approx 0.083$, $S\approx S_-\approx 0.0966$, i.e., they become equal to those expected from a "uniform" distribution [3,8,9].

Finally, we further comment on the results obtained from the on-off intermittency model. First, note that Fig. 5(a) indicates that S is probably larger than S_-, while in the fBm time series (Fig. 4) no definite sign for $S-S_-$ could be obtained. Second, in Fig. 5(b), we plot the fluctuations δS and δS_- (i.e., the standard deviations of the entropies S and S_-, respectively) vs $(\alpha-e)N^{1/2}$. It is clearly seen that these fluctuations are dramatically enhanced as the *critical* value is approached (i.e., $\alpha\rightarrow e$). This is strikingly reminiscent of our earlier results [5,6] upon analyzing electrocardiograms in natural time domain and studying the so-called QT intervals (see Fig. 1 of Ref. [6]). These results showed that the fluctuations of the entropy δS(QT) are appreciably larger in sudden cardiac death individuals than those in truly healthy (H) humans (see Fig. 2 of Ref. [6]). We emphasize, however, that this similarity should not be misinterpreted as stating that the simple logistic map model treated here can capture the complex heart dynamics, but only can be seen in the following frame: Since sudden cardiac arrest (which may occur even if

the electrocardiogram looks similar to that of H) may be considered as a dynamic phase transition [5,6], it is reasonable to expect that the entropy fluctuations significantly increase upon approaching the transition.

VI. CONCLUSIONS

In summary, recently recorded electric signals (having the largest amplitudes recorded to date) exhibit the property that both S and S_- are smaller than S_u and hence we conclude (when also considering that their κ_1 values are close to $\kappa_1 = 0.070$) that they are likely SES activities (critical dynamics). This property seems to stem from their infinitely ranged long-range temporal correlations as supported by computational results in fBm time series. The same property is found in calculations for a simple on-off intermittency model in which the signal amplitudes obey power law distribution (thus having a feature similar, in principle, with seismicity). The latter model also suggests that the fluctuations (δS and δS_-) significantly increase upon approaching the transition, which is strikingly reminiscent of the increased δS values found for the QT intervals for the sudden cardiac death individuals.

After the submission of the present paper, three strong earthquakes of magnitude 6.0 units occurred (a fact which is *extremely* unusual) in the Aegean sea at a distance only 100 km from the MYT station, thus confirming experimentally the classification of the intense signals M_1 to M_4 [Figs. 1(a) and 1(b)] as SES activities (critical dynamics). Two of these earthquakes occurred on 17 October 2005 and a third one on 20 October 2005. Interestingly, if we monitor the order parameter of seismicity suggested in Ref. [7], the time-window of the initiation of the strong earthquake activity on 17 October 2005 is determined with good accuracy, as described in Ref. [16]. Since in that area a *single* earthquake of magnitude 6.0-units occurs after a long time, i.e., on the average after a period of a few tens of years [43], the probability that these events, i.e., the SES activities and the (three consecutive strong) earthquakes, occurred as random events is found [16] (when taking into account the time elapsed between them) to be drastically smaller than 5%.

ACKNOWLEDGMENTS

We would like to express our thanks to V. Hadjicontis for his collaboration in keeping the MYT station in continuous operation.

[1] R. Yulmetyev, P. Hängii, and F. Gafarov, Phys. Rev. E **62**, 6178 (2000).
[2] R. Yulmetyev, F. Gafarov, P. Hängii, R. Nigmatullin, and S. Kayamov, Phys. Rev. E **64**, 066132 (2001).
[3] P. A. Varotsos, N. V. Sarlis, and E. S. Skordas, Practica of Athens Academy **76**, 294 (2001).
[4] P. A. Varotsos, N. V. Sarlis, and E. S. Skordas, Phys. Rev. E **66**, 011902 (2002).
[5] P. A. Varotsos, N. V. Sarlis, E. S. Skordas, and M. S. Lazaridou, Phys. Rev. E **70**, 011106 (2004).
[6] P. A. Varotsos, N. V. Sarlis, E. S. Skordas, and M. S. Lazaridou, Phys. Rev. E **71**, 011110 (2005).
[7] P. A. Varotsos, N. V. Sarlis, H. K. Tanaka, and E. S. Skordas, Phys. Rev. E **72**, 041103 (2005).
[8] P. A. Varotsos, N. V. Sarlis, and E. S. Skordas, Phys. Rev. E **67**, 021109 (2003).
[9] P. A. Varotsos, N. V. Sarlis, and E. S. Skordas, Phys. Rev. E **68**, 031106 (2003).
[10] P. A. Varotsos, N. V. Sarlis, H. K. Tanaka, and E. S. Skordas, Phys. Rev. E **71**, 032102 (2005).
[11] P. Varotsos, *The Physics of Seismic Electric Signals* (TERRAPUB, Tokyo, 2005).
[12] S. Abe, N. V. Sarlis, E. S. Skordas, H. K. Tanaka, and P. A. Varotsos, Phys. Rev. Lett. **94**, 170601 (2005).
[13] B. Lesche, J. Stat. Phys. **27**, 419 (1982).
[14] B. Lesche, Phys. Rev. E **70**, 017102 (2004).
[15] N. Scafeta and B. J. West, Phys. Rev. Lett. **92**, 138501 (2004).
[16] See EPAPS Document No. [E-PLEEE8-73-134603] for additional information. This document can be reached through a direct link in the online article's HTML reference section or via the EPAPS homepage (http://www.aip.org/pubservs/epaps.html).
[17] P. Bak, C. Tang, and K. Wiesenfeld, Phys. Rev. Lett. **59**, 381 (1987).
[18] P. Bak and C. Tang, J. Geophys. Res. **94**, 15635 (1989).
[19] X. Yang, S. Du, and J. Ma, Phys. Rev. Lett. **92**, 228501 (2004).
[20] R. Woodard, D. E. Newman, R. Sanchez, and B. A. Carreras, Phys. Rev. Lett. **93**, 249801 (2004).
[21] X. Yang, S. Du, and J. Ma, Phys. Rev. Lett. **93**, 249802 (2004).
[22] S. C. Jaume and L. R. Sykes, Pure Appl. Geophys. **155**, 279 (1999).
[23] L. R. Sykes, B. E. Shaw, and C. H. Scholz, Pure Appl. Geophys. **155**, 207 (1999).
[24] D. Sornette, *Critical Phenomena in the Natural Sciences: Chaos, Fractals, Selforganization, and Disorder: Concepts and Tools* (Springer-Verlag, Berlin, 2000).
[25] I. G. Main and F. H. Al-Kindy, Geophys. Res. Lett. **29**, 251 (2002).
[26] S. Padhy, Geophys. J. Int. **158**, 676 (2004).
[27] P. A. Varotsos, N. V. Sarlis, and E. S. Skordas, Phys. Rev. Lett. **91**, 148501 (2003).
[28] P. Varotsos and M. Lazaridou, Tectonophysics **188**, 321 (1991).
[29] A. Weron, K. Burnecki, S. Mercik, and K. Weron, Phys. Rev. E **71**, 016113 (2005).
[30] S. Mercik, K. Weron, K. Burnecki, and A. Weron, Acta Phys. Pol. B **34**, 3773 (2003).
[31] G. Samorodnitsky and M. S. Taqqu, *Stable Non-Gaussian Random Processes: Stochastic Models with Infinite Variance* (Chapman & Hall/CRC, Florida, 1994).
[32] B. Mandelbrot and J. R. Wallis, Water Resour. Res. **5**, 243

(1969).
[33] J. Szulga and F. Molz, J. Stat. Phys. **104**, 1317 (2001).
[34] B. B. Mandelbrot, *Gaussian Self-Affinity and Fractals* (Springer-Verlag, New York, 2001).
[35] M. Frame, B. Mandelbrot, and N. Neger, fractal geometry, Yale University, available from http://classes.yale.edu/fractals/, see http://classes.yale.edu/Fractals/RandFrac/fBm/fBm4.html
[36] C.-K. Peng, S. V. Buldyrev, S. Havlin, M. Simons, H. E. Stanley, and A. L. Goldberger, Phys. Rev. E **49**, R1685 (1994).
[37] S. V. Buldyrev, A. L. Goldberger, S. Havlin, R. N. Mantegna, M. E. Matsa, C.-K. Peng, M. Simons, and H. E. Stanley, Phys. Rev. E **51**, 5084 (1995).
[38] Y. Pomeau and P. Manneville, Commun. Math. Phys. **74**, 189 (1980).
[39] C. Toniolo, A. Provenzale, and E. A. Spiegel, Phys. Rev. E **66**, 066209 (2002).
[40] N. Platt, E. A. Spiegel, and C. Tresser, Phys. Rev. Lett. **70**, 279 (1993).
[41] J. F. Heagy, N. Platt, and S. M. Hammel, Phys. Rev. E **49**, 1140 (1994).
[42] N. J. Balmforth, A. Provenzale, E. A. Spiegel, M. Martens, C. Tresser, and C. W. Wu, Proc. R. Soc. London, Ser. B **266**, 311 (1999).
[43] See the United States Geological Survey (USGS) earthquake search web page http://neic.usgs.gov/neis/epic/epic.html for the relevant seismic catalogues.